2023-10-01

Optimal temperature-actuated control of a thermally-insulated roller blind

Hani Alkhatib
Technological University Dublin, d19126291@mytudublin.ie

Philippe Lemarchand
Technological University Dublin, philippe.lemarchand@tudublin.ie

Brian Norton
Tyndall National Institute, brian.norton@ierc.ie

See next page for additional authors

Recommended Citation

H. Alkhatib, P. Lemarchand, B. Norton, D.T.J. O'Sullivan, Optimal temperature-actuated control of a thermally-insulated roller blind, Build Environ. 244 (2023) 110751. DOI: 10.1016/j.buildenv.2023.110751

Funder: Science Foundation Ireland Research Centre for Energy, Climate, and Marine

Building and Environment 244 (2023) 110751

Contents lists available at ScienceDirect

Building and Environment

journal homepage: www.elsevier.com/locate/buildenv

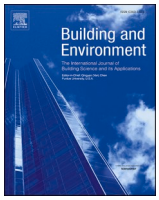

Optimal temperature-actuated control of a thermally-insulated roller blind

H. Alkhatib [a,b,c,*], P. Lemarchand [a,b,c], B. Norton [a,b,c,e], D.T.J. O'Sullivan [c,d]

[a] School of Electrical and Electronic Engineering, Technological University Dublin, Ireland
[b] Dublin Energy Lab, Technological University Dublin, Dublin, Ireland
[c] MaREI, The SFI Centre for Energy, Climate and Marine, Ireland
[d] Intelligent Efficiency Research Group, School of Engineering, University College Cork, Cork, Ireland
[e] International Energy Research Centre, Tyndall National Institute, University College Cork, Cork, Ireland

ARTICLE INFO

Keywords:
Roller blind
Dynamic thermal insulation
Adaptive façade
Heating, cooling and daylight
Occupant comfort

ABSTRACT

By altering the thermal equilibria between internal and ambient environments, dynamic insulation can minimize heating and cooling building energy requirements. The performance of a thermally-insulated roller blind was evaluated both experimentally and via simulation studies. The variation of blind position was optimized to minimize building energy consumption, maintain thermal comfort, and minimize daylight discomfort for a particular system, location and conditions. The roller blind was adjusted between four positions, from fully-open to fully-closed, optimal indoor temperature switching thresholds found for moving to these blind positions were 15 °C, 18.4 °C, 19.4 °C and 21.4 °C, respectively. Using these resulted in a 15.3% energy savings and a 7% reduction in occupancy daylight discomfort compared with no blind.

1. Introduction

The 40% of global primary energy consumption associated with the operation of buildings produced 10 $GtCO_2$, accounting for 28% of global energy-related CO_2 emissions in 2020 [1,2]. Decarbonising buildings is thus an important goal [3]. Buildings facades mediate between outdoor and indoor environments. When the parameters of that mediation are fixed, occupant comfort is met solely by the provision of heating and cooling systems. In shallow-plan buildings, adaptive facades that can alter their thermophysical properties can contribute to the achievement of indoor comfort conditions with low energy use [1,4,5], as less heating and cooling is required.

Dynamic insulation can reduce the amount of energy needed to heat and cool a building by changing the thermal equilibrium between the interior and exterior environments. Both experimental and simulation examinations were conducted to evaluate the effectiveness of a thermally insulated roller blind. The change of blind position was optimized to reduce the energy consumption of the building, maintain thermal comfort, and reduce daylight discomfort.

A window's specification, dimensions, shape, orientation and windowsill height can significantly affect the daylight transmitted and glare [31,32]. In this study, a full room height window has been considered. These feature in many office and industrial buildings and houses, particularly where facades look out to private spaces. This is because privacy can be maintained whilst external views are available to occupants located more deeply into a room than would be the case with a half-room height window [33]. A typical double-glazed window is employed to provide results relevant to the introduction of insulated roller blinds into a currently existing building.

2. Relevant previous research

Insulating a building fabric reduces energy consumption when ambient temperatures are low by reducing heat loss. In heating-dominated climates, high levels of thermal insulation are thus typically mandated by building regulations, standards and codes. This has led to the development and commercialization of high-performance thermal insulation technologies [6–9]. However, the benefits of high levels of thermal insulation in winter can also result in overheating in summer that can then incur or increase cooling energy consumption depending on a building's location, type, construction, façade orientation and density and pattern of occupancy [10].

Altering the thermal equilibria between internal and ambient environments can minimize both heating and cooling building energy requirements. Several researchers have thus investigated the possibility of using adaptive "Dynamic Insulation Systems" (DIS) in building

* Corresponding author. School of Electrical and Electronic Engineering, Technological University Dublin, Ireland.
E-mail address: d19126291@mytudublin.ie (H. Alkhatib).

https://doi.org/10.1016/j.buildenv.2023.110751
Received 4 June 2023; Received in revised form 9 August 2023; Accepted 18 August 2023
Available online 22 August 2023

Table 1
Techniques used to alter facade thermal insulation.

Technology	Operation	Location on facade	Advantages	Disadvantages	Reference
Removable insulation	Removing and replacing insulation boards physically	Wall	Readily controls heat gain fluctuations.	Hand-operated and time-consuming.	[16,17]
Dynamic insulation of wall cavity	Using foam beads to fill/unfill a wall cavity.	Wall and window	Achieves high thermal resistance switching	Complex control, large thickness.	[6]
Translucent wall element with switchable U - and g -value	Movable translucent insulation panel inside a closed cavity	Wall	Controls the heat flow in the façade element.	Cannot be readily integrated into existing buildings.	[18]
Hydronic insulation	Fluid flows inside a U-pipes system with a variable mass flow rate and variable supply temperature	Wall	Significantly reduces the heating energy demand of a building.	Cannot be readily integrated into existing buildings, complex system with high initial and running costs.	[19]
Cellular insulation	Thin polymer membranes are positioned within a wall to create layers that expand and collapse.	Wall	Effective for thermal management over a large temperature range.	Requires active maintenance, and complex control.	[20]
Ventilation within insulation layers	Insulating expanded polystyrene separated from the internal wall by a channel that can be ventilated.	Wall	Reduces the energy demand of the building in summer periods.	Complicated to install in existing buildings.	[21]
Gas pressure variation	U-value is varied by changing internal pressure in nano-porous insulation material	Wall	Effective in buildings where the energy used for cooling is more than the energy used for heating.	Complex system and requires active supervision.	[22]
Gas-filled panels	Barrier foil and baffle structure inside a variable gas-filled panel.	Wall	Low thermal conductivity,	Expensive and requires active monitoring.	[23]
Nano insulated materials	Physically installing different types of aerogel-based thermal superinsulation to fill cavities.	Wall	Low thermal conductivity.	Expensive and complicated to install in existing buildings.	[24]
Phase change materials	Switchable phase change material system coupled with thermal insulation	Window	Reduces the energy peak demand and indoor temperature fluctuations.	Early-stage technology with complex parts and control.	[25]
Phase changing material	Switchable phase change material system coupled with thermal insulation	Window	Reduces the energy peak demand and indoor temperature fluctuations.	Early-stage technology with complex parts and control.	[26]
Thermally insulated roller blind	Insulated roller blind moves inside the window frame.	Window	Cheap, large range of control over daylight and thermal conductivity of the window and can be integrated into existing buildings.	Requires active maintenance.	This study

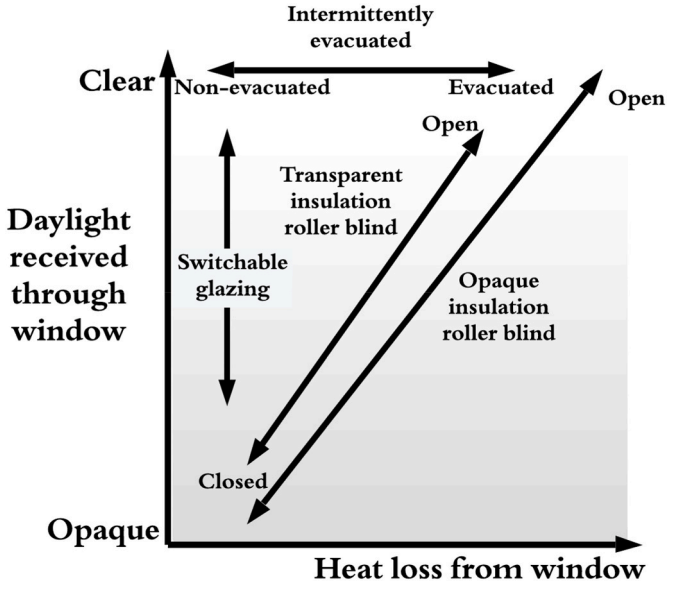

Fig. 1. Heat loss and optical transmission using different facade technologies.

envelopes whose time-varying thermal properties may provide controllable thermal insulation. Pflug et al. [11] presented a translucent wall with a switchable heat loss coefficient, provided by an element positioned vertically inside a double-glazed window. For the particular conditions examined, this system achieved a 29.6% cooling energy demand reduction. Dabbagh and Krarti [12] found experimentally that rotatable insulated shading gave 8.3%, 11.3%, and 11.4% savings in annual HVAC energy consumption in Golden, Colorado; Phoenix, Arizona and San Francisco, California, respectively. Maurer et al. [13] reported that a variable heat loss coefficient translucent wall element, arranged to roll-up and roll-down within a glazed closed cavity could avoid overheating. For dynamic insulation of opaque walls operated with fully-on or fully-off settings, Park et al. [14] found a 30% reduction in cooling energy for buildings in Golden, Colorado and Madison, Wisconsin. Menyhart and Krati [15] found variable heat loss coefficient façade systems for residential buildings could achieve up to 45% heating and cooling energy savings for a range of locations also in the United States of America. The various studies summarized in Table 1 illustrate the diverse breadth of approaches that have been examined to achieve dynamic insulation of building facades.

As indicated in Table 1, dynamic insulation systems can either alter (i) the heat loss of a wall or (ii) the heat loss and daylight provided by a window. Fig. 1 indicates the range of control over the heat loss and the daylight received associated with selected technologies. As windows are the component with the highest heat loss in most façades, enabling their level of thermal insulation to adapt to prevailing conditions can contribute to reducing annual heating and cooling requirements. However, avoiding a concomitant (i) increase in artificial lighting, energy consumption and (ii) loss of the benefits associated with exposure to daylight [27,28], requires optimal control of the deployment of dynamic thermal insulation at windows.

Overall, most dynamic insulation systems presented in previous studies have been (i) inflexible and hard to install in existing buildings and (ii) not applicable to glazed elements of facades. Most technologies intended for facade walls to control heat transfer, cannot address control of daylight nor, obviously, have any effect on occupant's daylight comfort [29,30].

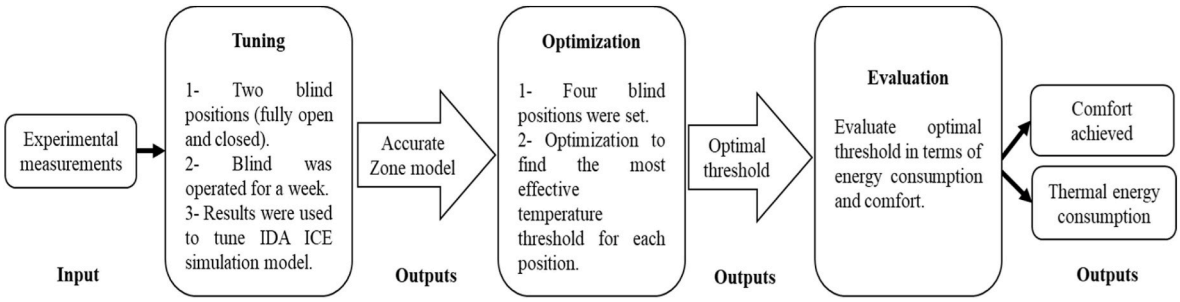

Fig. 2. Key steps of the methodology outlined.

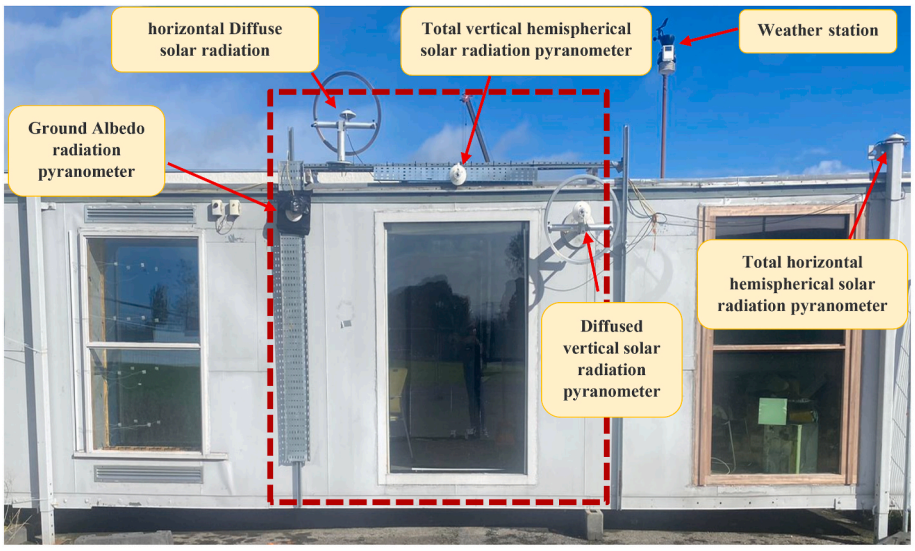

(a)

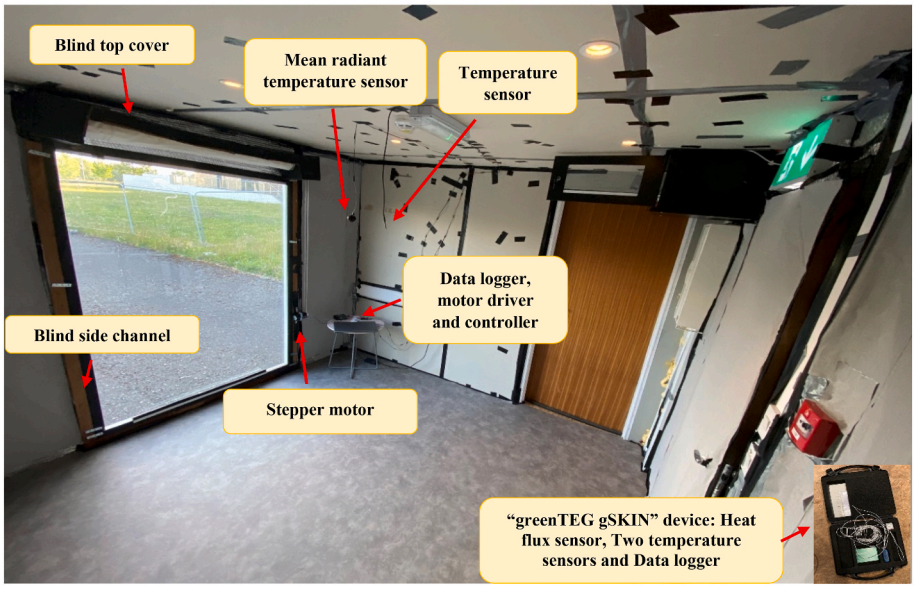

(b)

Fig. 3. (a) Test room exterior, (b) Test room interior.

Both roller blinds and Venetian blinds can be insulated. Tightly sealing the slats of a Venetian blind and the overall assembly into a frame to avoid loss of air trapped between the blind and window glass is very difficult to achieve and maintain. There are also inherent limitations on the control of a Venetian blind [29,30]. As indicated in Fig. 1, roller blinds can achieve a high range of control over both heat loss and daylight through a window. Despite this, controlling heat loss and optical transmittance with an insulated roller blind has rarely been explored. In this study, a dynamic insulating roller blind that modulates both heat transfer and daylight is examined, this was done using

Table 2
Properties of solar test cell fabric.

Fabric element	U-Value (W/m^{2}K)	Area (m^2)
External Wall	0.30	6.58
Internal Wall	0.45	6.58
Roof	0.38	8.34
Floor	0.56	8.34
Doors	1.16	2.00
Glazing	2.98	3.29
Glazing Frame	0.83	0.05
Insulated Blind	1.38	3.29

simulation and physical experiments (which were used as a calibration process). The energy saving and daylight comfort that can be achieved by this system was investigated. This study represents environmental control strategies involving blinds, while also providing a broader perspective that extends beyond the specifics of the physical system under examination.

3. Methodology

The three stages of the methodology used are summarized in Fig. 2.

Initially, in the "tuning" stage, a thermally-insulated roller blind was operated experimentally in a full-scale outdoor test cell for a week. Measurements of (i) outside weather conditions and (ii) indoor air temperatures, mean radiant temperature and illuminance were made. These were used to tune a simulation of the test cell in IDA ICE [34,35]. dynamic building simulation software by comparing the measurements with model outputs.

Then, in an "optimization" stage, the model built in IDA ICE was used to determine the optimal temperature threshold for each different blind position in terms of energy consumption.

Finally, in an "evaluation" stage, the optimal control strategy from the optimization stage was evaluated in terms of energy consumption and thermal and daylight comfort.

4. Experiments

The experimental test cell, shown in Fig. 3, is located in Dublin (53.3° N, 6.26° W). comprised a 3 m × 2.7 m x 3 m south-facing cuboid room whose exterior is delineated by the dashed red line.

Outside the test cell six pyranometers measured total hemispherical, diffused and ground albedo solar radiation on the horizontal and south-facing vertical planes. A weather station measured ambient temperature, humidity, dew point, atmospheric pressure, wind direction and wind speed. Inside the test cell room, mean air temperature and mean radiant temperature were measured. All measurements were recorded at 15-min intervals.

The overall heat loss coefficient of the test cell fabric was measured using a "greenTEG gSKIN" device shown in Fig. 3, that consisted of two temperature sensors (one for each side of the test cell fabric) and a heat flux sensor. Measurements of the heat loss coefficient of each fabric element were taken over three days. Measured heat loss coefficients of fabric elements are shown in Table 2.

For daylight measurements within the test cell room, a High Dynamic Range (HDR) EOS 200D camera mounted in the corner of the room paired with a lux meter were used. The camera lens was calibrated using Aftab Alpha Software; the use of this software in this application has been validated in previous research [36–38]. Three steps were taken to process images from the camera,

(i) Calibration of the lens, where a total of six images were taken at the same time at two different angles while measuring the luminous intensity using the lux meter. The images were then uploaded to the Aftab Alpha software for lens calibration,
(ii) Images processing, images of the solar test cell interior were then taken four times a day during the tuning week,
(iii) Images were then processed inside the software to give the luminous intensity for the whole room. A lux meter gave luminous intensity readings on two points on each image.

Table 3 summarizes the accuracy, range and measurement interval of the instruments used in this study.

4.1. Thermally-insulated roller blind

A 1.50 m × 2.20 m opaque thermally insulted roller blind, was fabricated using a foldable insulation material as shown in Fig. 4. It was mounted on the inner side of the windowpane. Side channels on the window frame ensured the blind remained closely adjacent to the glass while moving up or down. A cover at the top of the blind minimized air leaks from between the glass and the insulated blind. The insulated blind is operated by "Nima 23" stepper motor, "Arduino" controller and motor driver. The motor was powered by a 24 V 6 A power supply with the controller powered by a 5 V 1 A power supply. A data logger recorded when these movements occurred to enable the electricity consumption of the blind to be calculated.

5. Simulation model

IDA ICE software has been used for the simulation of building indoor environment and energy simulation [39–41]. The model of the room created in the IDA ICE software shown in Fig. 5 followed the dimensions of the solar test cell, the surrounding buildings (to take shading into account) and the measured overall heat loss coefficient of the room fabric and blind.

The test cell had three internal gains (i) LED lighting units of 350 W with an efficacy of 20 lm/W, lighting was set to maintain above 200 lx

Table 3
instruments accuracy range and measurements interval.

Measurement	Instrument	Accuracy	Range	Measurement interval
Temperature	Thermistor DS18B20	±0.5 °C	- 10 to 85 °C	5 min
	Thermistor DHT22 placed inside a black globe	±0.5 °C	- 40 to 80 °C	5 min
Illuminance	EOS 200D canon HDR camera Tondaj Lx- 1010B lux meter	±5%	0 to 50,000 lx	4-times a day
Solar Irradiance	"Class II" solar pyranometers	Depends on the calibration factor	0–2000 W/m^2	5 min
Overall heat loss coefficient	Temperature sensors	±0.5 °C	- 40 to 100 °C	1 min.
	Flux sensor	±0.11 W/m^2	±300 W/m^2	The kit was mounted at each fabric element for three days.

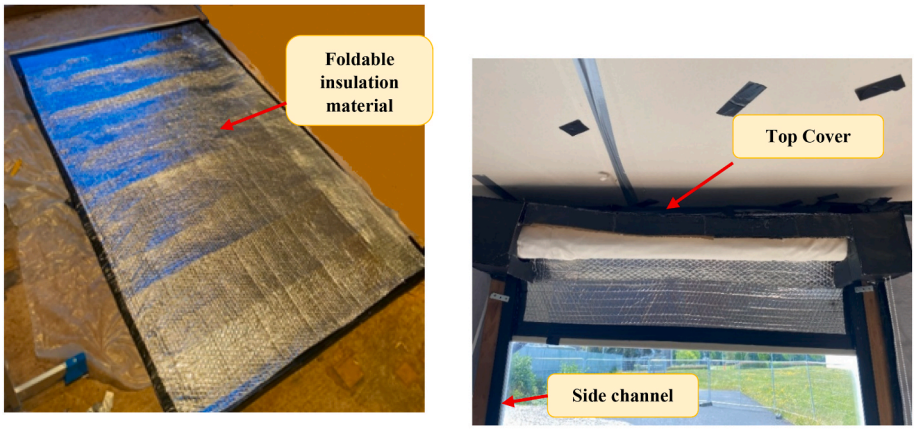

(a)

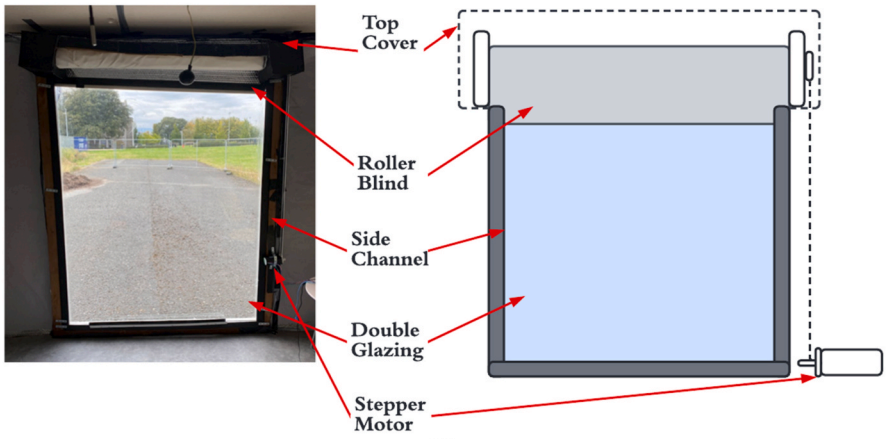

(b)

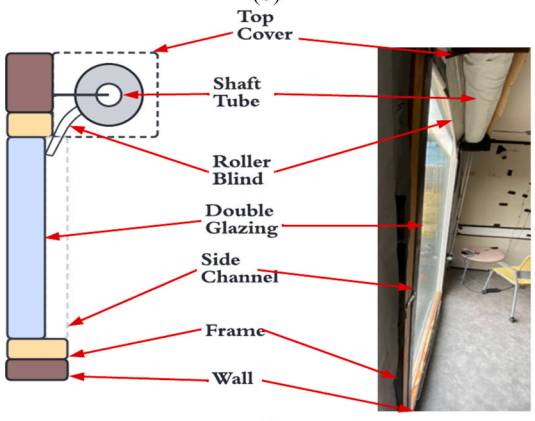

(c)

Fig. 4. (a) Foldable insulation material, top cover and side channels of the blind, schematic diagram of the dynamic shading system (b) Front view, (c) Side view.

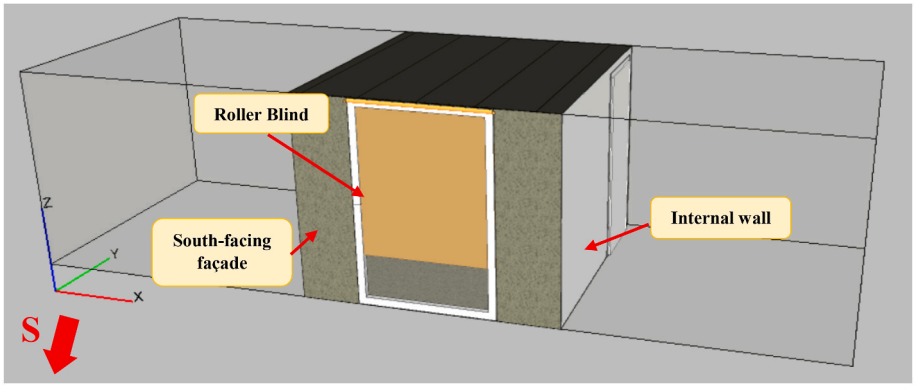

Fig. 5. Solar Test Cell model in IDA ICE.

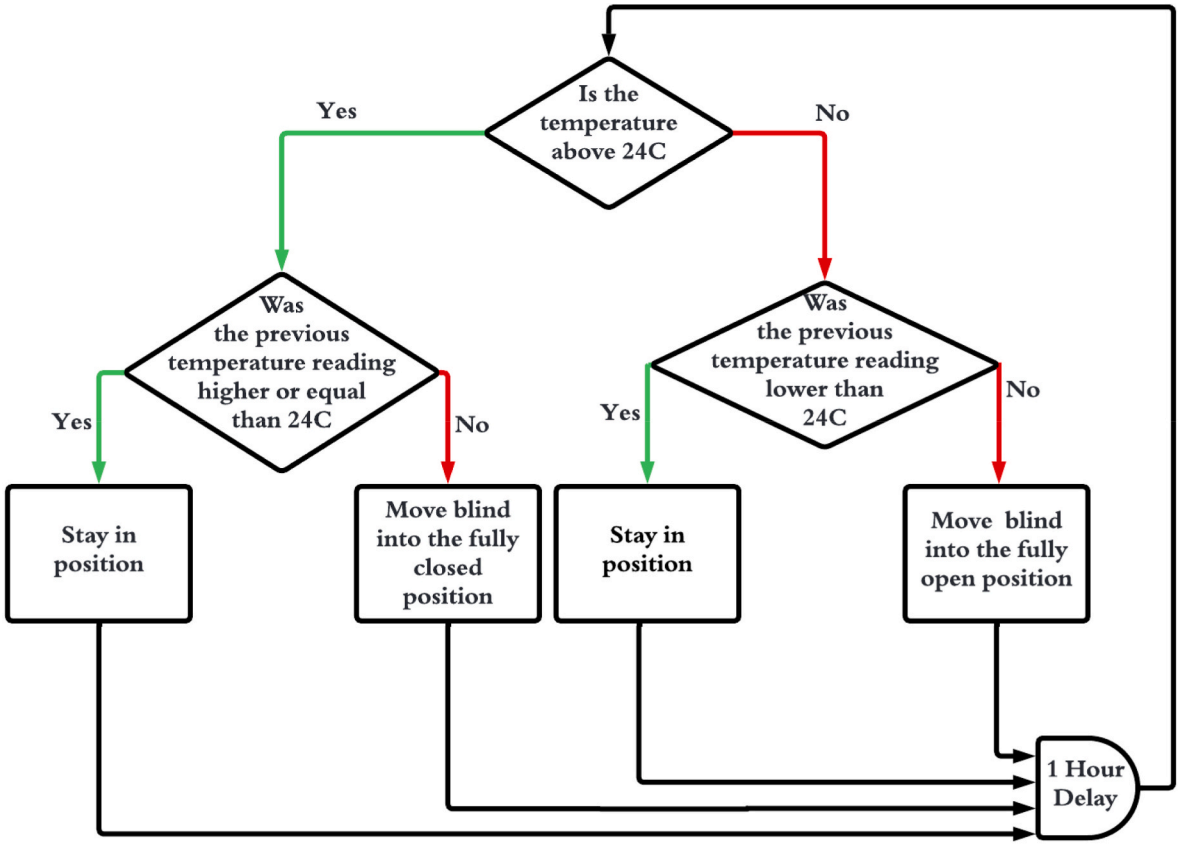

Fig. 6. Control strategy flow diagram used for tuning the simulation model.

turned off when 500 lx from daylight was reached. (ii) indoor equipment producing 200 W of heat and (iii) one occupant with a metabolic rate for each person is set to 1 Metabolic Equivalent of Task (MET). Thermal comfort levels were defined using ANSI/ASHRAE Standard 62.1 and ANSI/ASHRAE Standard 55 [46,47]. Lighting comfort levels were defined based on recommended standard illuminance levels in office workplaces [48,49]. Following this BSI standard, average illuminance in the zone must be within the 200–500 lx range at a height of 1.2 m above the floor level to ensure daylight comfort is maintained, and glare is limited [45,50]. The range identified in this BSI standard represents a conservative limit designed to avoid glare, however, this does not mean that illuminance levels above these limits will result in glare [49]. In this study, daylight comfort is calculated depending on the number of hours that the average illuminance is in the recommended range during work hours. Outside the scheduled occupancy time (09h–17h) and on weekends, there is no constraint on the indoor lighting and thermal comfort, meaning no lighting, heating and cooling energy consumption occurs, this could lead to low temperatures outside of working hours, which might lead to mould problems.

6. Procedure for tuning the simulation model

When tuning the simulation model, measured data was used where the blind was (i) controlled by an actuator solely receiving signals from the mean air temperature sensor in the room, and (ii) only in fully-open or fully-closed blind positions. When the temperature was below 24 °C the blind was set to remain in the fully-open position. When the temperature reached 24 °C the blind lowered to the fully-closed position. A flow chart illustrating this control strategy is shown in Fig. 6.

Four days' experimental data were used for tuning. Tuning was done

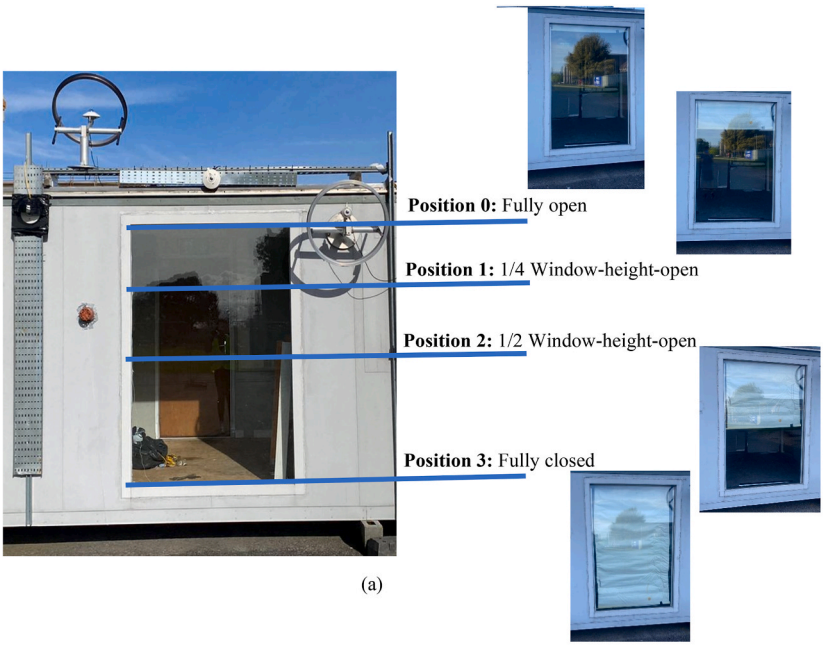

(a)

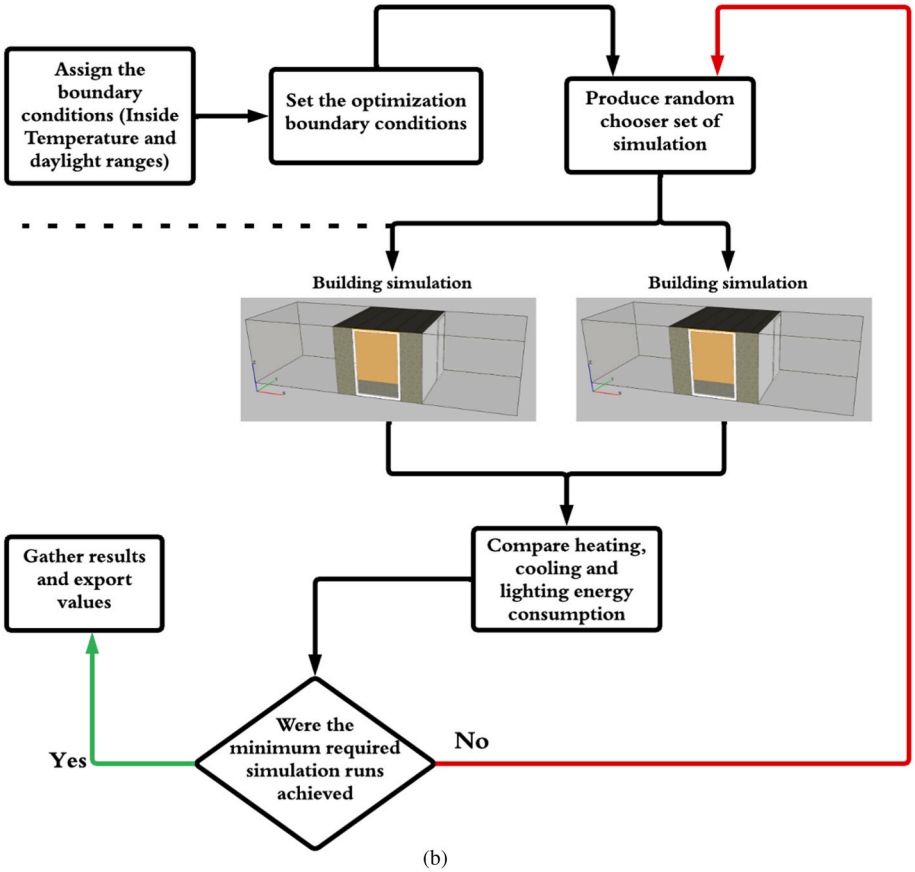

(b)

Fig. 7. (a) Roller blind positions examined (b) Optimization flow chart.

by importing the measured hourly dry-bulb temperature, solar radiation (direct normal radiation and diffuse radiation on horizontal and vertical surfaces), relative humidity, cloud cover, wind speed and direction inside the weather file of the IDA ICE model. To tune the thermal properties of the test cell simulation model, the thermal bridges' psi-values of that model were adjusted according to the measured inside mean air temperatures and but they were not considered as time-varying parameters. Three days' experimental data were used to validate the tuning. The measured inside mean air temperature and daylight were compared with the predicted air temperature and daylight from the IDA ICE model. The daylight properties of the double-glazed window did not require tuning as the measured illuminance levels over the test cell

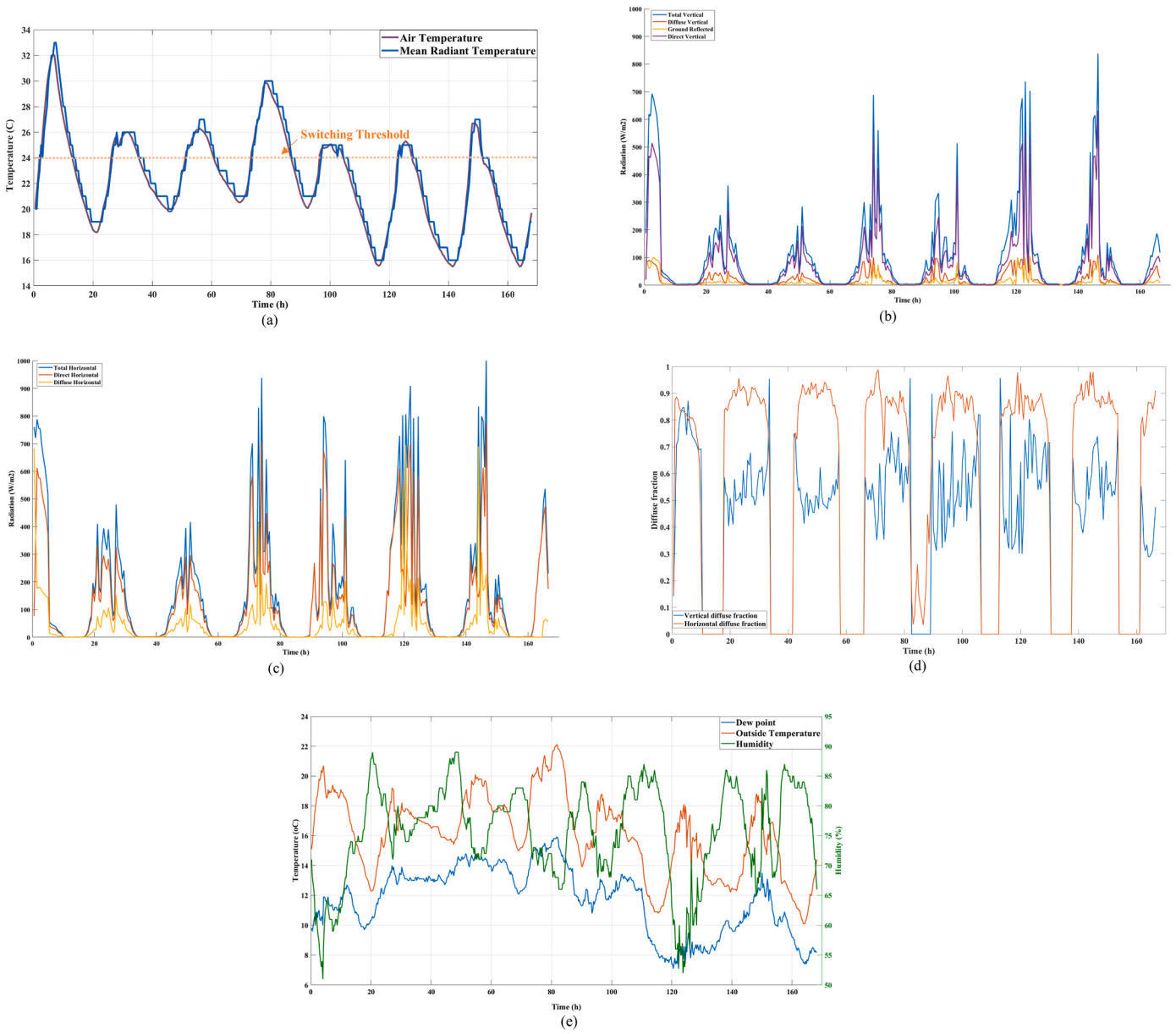

Fig. 8. (a) Measured indoor air temperature and mean radiant temperature, (b) measured solar radiation incident on the façade, (c) measured horizontal solar radiation, (d) diffuse fraction, (e) measured outdoor temperatures, dewpoints and relative humidity.

matched the predicted levels by the model. This study assumed no ventilation, the infiltration rates were low.

7. Procedure for determining optimal internal temperature threshold for moving the blind

Four different blind positions shown in Fig. 7 were selected and examined. An optimization process sought to find the optimal temperature at which to move the roller blind to four different positions. The optimization process was done by comparing simulations of the energy of the room produced by Monte Carlo statistical random sampling. Monte Carlo method has been widely used to treat optimization problems in building simulations [42–44]. The optimization objective was set to find the temperature threshold that minimized heating, cooling and lighting energy consumption of the room for each blind position. A flow chart of the optimization process is shown in Fig. 7. The blind positions were chosen because although the heat transfer varies linearly with the area of glazing insulated, the daylight behaviour is non-linear; little change in daylight penetration occurs between the 1/2 window-height-open and fully-closed blind positions [45].

Optimal temperature thresholds for blind operation achieved desired comfort conditions with the lowest heating, cooling and lighting energy consumption. The optimization simulation ran for one year using Dublin weather data from the ASHRAE IWEC2 database [51].

8. Results

8.1. Tuning of the simulation model

Indoor temperatures and mean radiant temperatures recorded from 20/Jun to 27/Jun are shown in Fig. 8 As can be seen, when closed, indoor temperatures did not rise when solar radiation incident on the façade and outdoor temperatures rose as shown in Fig. 8. The blind avoided overheating this has also been shown in previous studies of dynamic insulation systems [17,52]. While the blind was closed, indoor temperatures decrease was not significant even at night, indicating a low

(a)

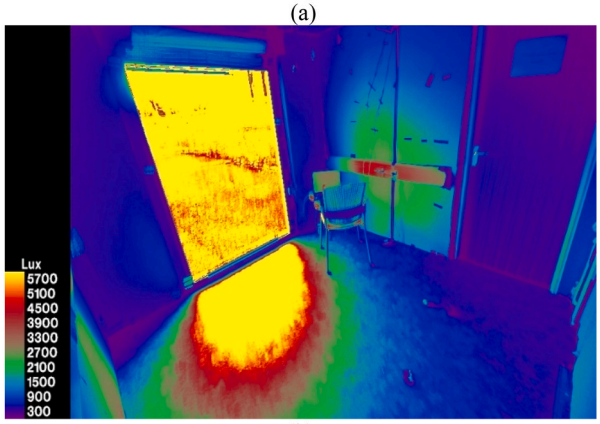

(b)

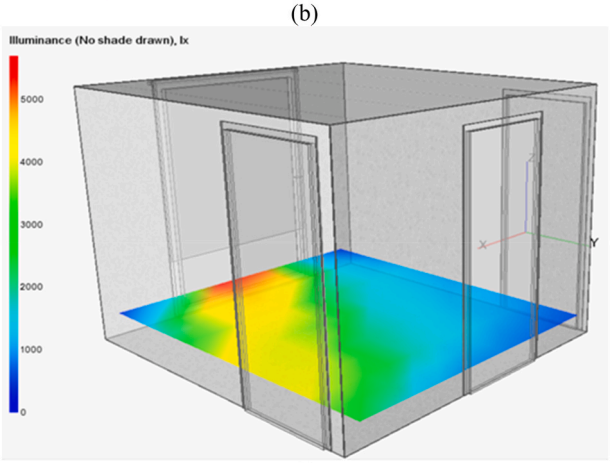

(c)

Fig. 9. Validation of the internal daylight (a) Solar test cell at 2:30pm (picture taken from HDR camera), (b) Measured lx level, (c) Predicted lx level.

rate of heat loss through the window. For daylight prediction validation, high-definition photographs were taken of the room interior four times a day for a week. Fig. 9 shows the room at 2:30 p.m. at day five of the week. Fig. 9 also shows predicted and measured luminous intensities for the blind fully-open. Good agreement can be seen in Fig. 9 between measured and predicted daylight. This means that no tuning was required for the optical properties of the window. The Normalized Root Mean Squared Error (NRMSE) between the simulated predicted temperatures and measured indoor temperatures was calculated. As shown in Fig. 10, the NRMSE was 0.78, meaning that the simulation model had predicted indoor temperature with 78% accuracy. The correlation between measured and predicted indoor air temperature was 0.89 as shown in Fig. 10. This means the tuning process produced low systematic and random errors.

8.2. Optimal internal temperature threshold for moving blind

For the Monte Carlo sampling, 500 annual simulations were conducted. The indoor temperature threshold that resulted in minimum annual heating, cooling and lighting energy needs was then used for placing the blind at each of the four selected positions. The optimization was bounded within an internal temperature range of 15 °C–25 °C. meaning that during the optimization temperatures in that range was chosen randomly to simulate the energy consumption. Whilst maintaining comfort conditions, the optimization procedure explained in Section 7, calculates the resultant energy consumptions for each temperature threshold. Table 4 shows temperature thresholds for each insulated roller blind position that gave the least energy needs and the corresponding overall heat loss coefficient of the window aperture at each position. The optimization showed that temperature thresholds at the higher and lower ends of the chosen temperature range resulted in a high annual energy consumption.

The yearly heating, cooling, lighting and blind energy consumptions shown in Fig. 11 were 1716 kWh, 952 kWh, 64 kWh and 242 kWh respectively. The lighting consumption is low since the working hours considered were mostly within the daytime. When the blind is left in the fully-open position as shown in Fig. 11, heating, cooling and lighting energy consumptions were 1743 kWh 1636 kWh and 50 kWh, respectively. Optimal insulated roller blind positioning that resulted in a 15.3% energy saving when compared with no blind.

As expected, the lighting energy consumption increased with the blind in optimal positions because when the blind is fully-closed (especially in summer) no daylight obviously enters the room, so artificial lighting solely provides the luminous intensity required. The percentage saving in cooling energy consumption was higher than the percentage saving of heating consumption since the temperature increases moved the blind to move to position(s) that (i) decreased solar heat gain, and (ii) decreased the heat loss rate from the part of the window covered by the blind from 2.98 W/m^2K to 1.60 W/m^2K, thus internal temperature rose after the blind moved to cover more of the window.

9. Discussion

Daylight discomfort was reduced by 7% (from 26% using fully open position to 19% using the optimized threshold) over the year with the blind in the optimized positions compared with the blind permanently in the fully open position. Fig. 12 shows the number of hours in which the blind stayed at each position to achieve the optimal internal condition. The blind remained mostly fully-open during the night when the heating and cooling systems were off. Fig. 13 shows the internal temperature of the test cell room at 15 min intervals during working hours (9 a.m.–5 p.m., Monday to Friday) over the year. It can be seen that the indoor temperature remained within the comfort range. The median air temperature is represented by the dark blue line in the box. The light blue boxes, dash lines, and individual points represent the interquartile ranges (IQR), the whisker limits (1.5 times the IQR), and outlier air temperatures respectively. In the summer months, the average internal air temperature of the room was higher (compared to winter months), so the blind was often in lower positions.

Solar load ratio is the ratio between solar energy available at a façade and building energy demand. Correlations of solar load ratio to a fraction of overall energy requirement met by harnessing incident solar energy enable generalized performance comparison of different solar heating and cooling technologies [53–55]. The relation of monthly solar heating fractions with monthly solar load ratios for a window using the insulated roller blind and the same window without it shown in Fig. 14 shows use of the blind did not significantly reduce the overall amount of solar gain harnessed when averaged over a month. Notably though the insulated roller blind gave better hour-by-hour comfort conditions seen in Fig. 13.

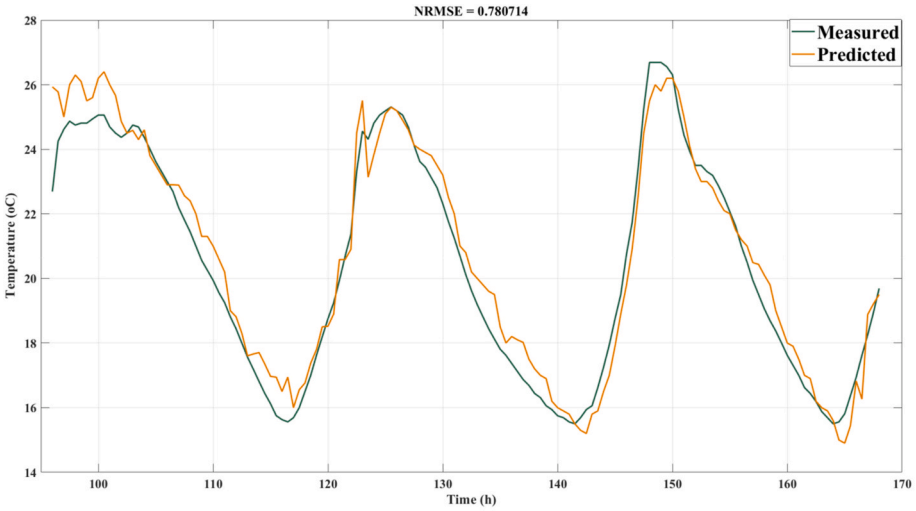

(a)

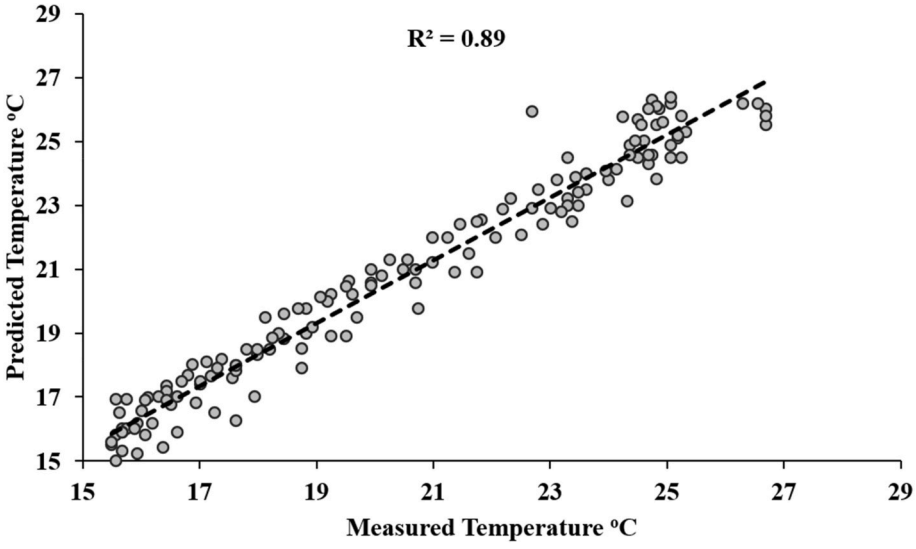

(b)

Fig. 10. (a) Validation of the tuning by comparing measured and simulated indoor temperature over three days, (b) Comparison of measured and predicted hourly indoor air temperatures for three days.

Table 4
Optimal temperature threshold with corresponding blind positions.

Temperature threshold °C	U-value of window aperture (W/m^2K)	Corresponding Roller Blind Position
<18.3	2.98	Fully open (Position 0)
18.3	2.64	Quarter height Position (Position 1)
19.3	2.29	Mid height position (Position 2)
>21.4	1.60	Fully closed (Position 3)

10. Conclusion

Controlling the adjustment of thermally insulated roller blind between four different positions controlled using optimal internal temperature threshold can help avoid overheating in summer and lowers heat loss at night. For the particular system and conditions studied, these temperature thresholds were 15 °C, 18.4 °C, 19.4 °C and 21.4 °C for fully-open, quarter height, mid-height and dully-closed positions, respectively. The optimally controlled thermally insulated roller blind achieved a 15.3% overall energy saving for heating, cooling and lighting, and an increase of 7% in time of daylight comfort over the year compared to a window with no blind. This study provides a methodology for determining temperature-actuated control of an insulated roller blind that can be applied to a range of climates and occupancy conditions. The deployment of insulated roller blinds with optimal control is recommended to reduce building energy use, particularly as part of the energy refurbishment of existing buildings.

The particular results presented only apply to the particular climate, occupancy conditions, building fabric and heat loss coefficient of the insulated blind used in the case study. This study only looked at simulations during working hours. This means that low internal temperature was not included in the threshold optimization also the presumed omission of ventilation means that beyond the specifics of climate and building type, the findings are strongly tied to the assumption of a

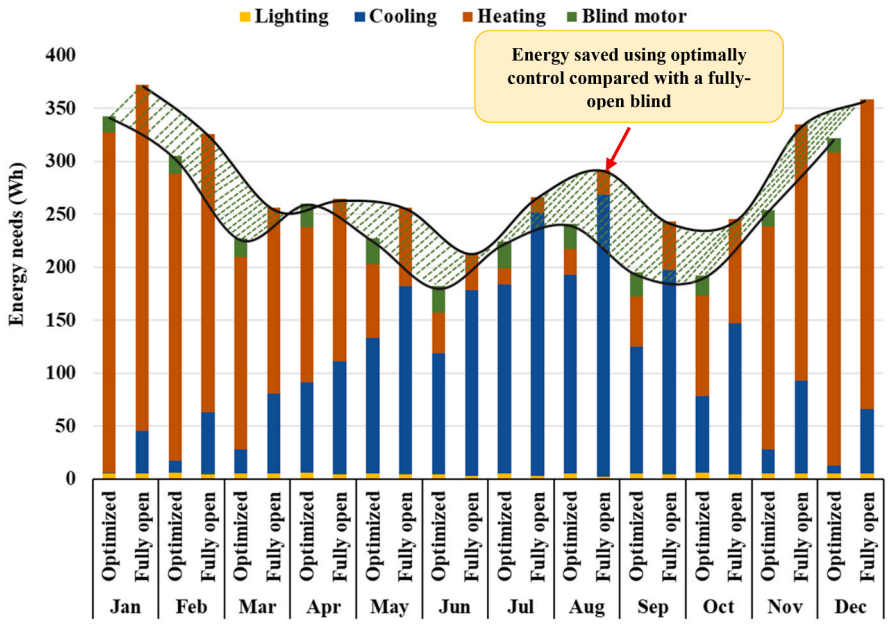

Fig. 11. Heating, cooling, lighting and blind's motor energy consumptions using optimized switching thresholds and a permanently fully open blind.

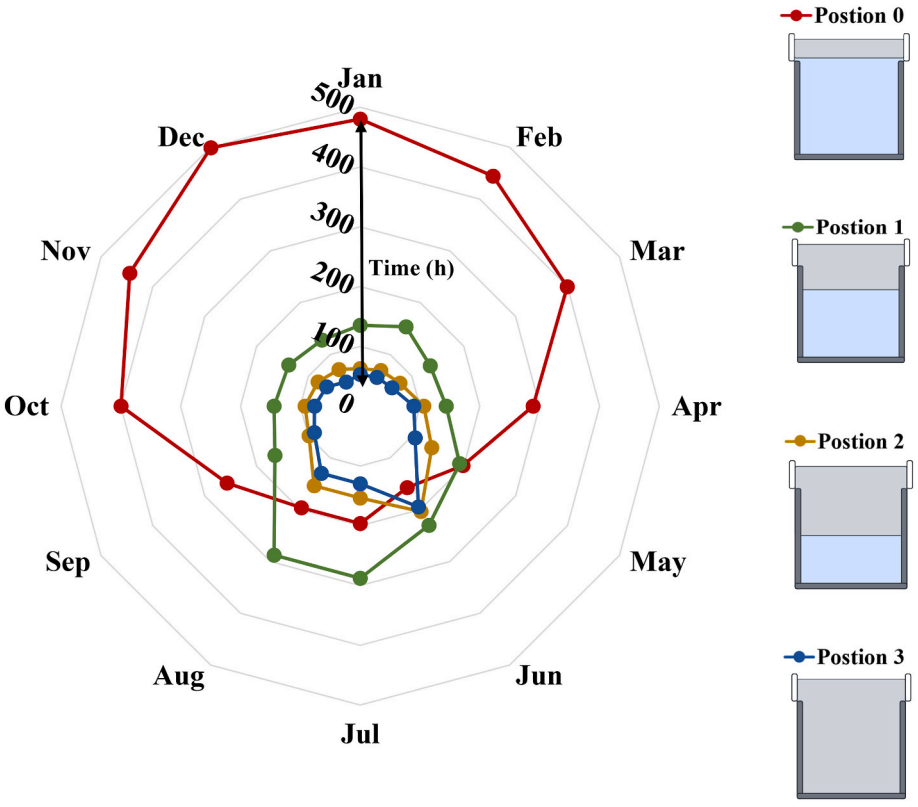

Fig. 12. Number of hours spent by the blind at each position when optimally controlled over daylight period for each month.

mechanically controlled environment. Future studies should investigate the benefits of using variable thermal insulation during non-working hour. Future studies should also investigate how far a multi-room scenario can be optimized especially in situations where rooms have clear schedules.

CRediT authorship contribution statement

H. Alkhatib: Writing – original draft, Visualization, Software, Resources, Methodology, Investigation, Formal analysis, Data curation, Conceptualization. **P. Lemarchand:** Writing – review & editing, Validation, Supervision, Project administration, Methodology, Investigation, Formal analysis, Data curation, Conceptualization. **B. Norton:**

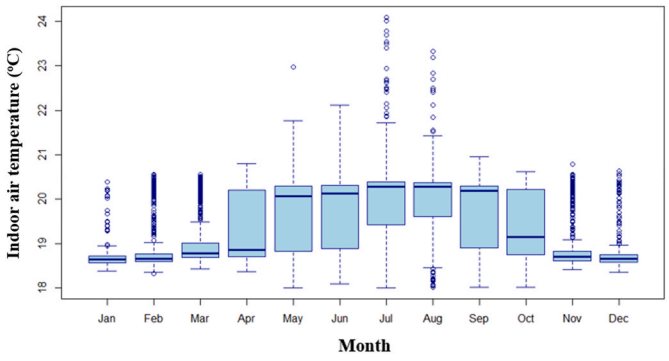

Fig. 13. Indoor air temperature during working hours over the year with adaptive insulated blind.

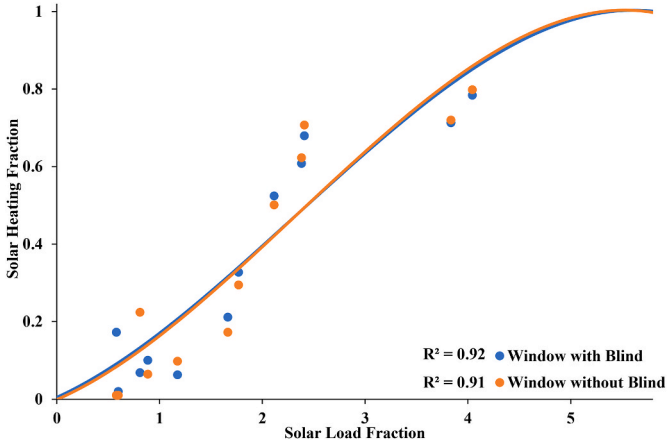

Fig. 14. Correlation Monthly solar load vs monthly solar heating fraction.

Writing – review & editing, Validation, Supervision, Resources, Project administration, Methodology, Investigation, Funding acquisition, Formal analysis, Data curation, Conceptualization. **D.T.J. O'Sullivan:** Writing – review & editing, Validation, Supervision, Project administration, Investigation, Funding acquisition, Data curation, Conceptualization.

Declaration of competing interest

The authors declare that they have no known competing financial interests or personal relationships that could have appeared to influence the work reported in this paper.

Data availability

Data will be made available on request.

Acknowledgment

This research was funded by MaREI, the SFI Research Centre for Energy, Climate, and Marine [Grant No: 12/RC/2302_P2]. The author acknowledges the assistance of Max Tillberg of the EQUA Solutions support team in the development of the simulation model used in the study.

References

[1] H. Alkhatib, P. Lemarchand, B. Norton, D.T.J. O'Sullivan, Deployment and control of adaptive building facades for energy generation, thermal insulation, ventilation and daylighting: a review, Appl. Therm. Eng. (2020), 116331, https://doi.org/10.1016/j.applthermaleng.2020.116331.

[2] United Nations Environment Programme, 2020 global status report for buildings and construction: towards a zero-emission, efficient and resilient buildings and construction sector, Nairobi (2020). https://globalabc.org/sites/default/files/inline-files/2020 buildings gsr_full report.pdf.

[3] B. Norton, W.B. Gillett, F. Koninx, Briefing: decarbonising buildings in Europe: a briefing paper, Proceedings of the Institution of Civil Engineers - Energy 174 (2021) 147–155, https://doi.org/10.1680/jener.21.00088.

[4] G. Capeluto, C.E. Ochoa, Intelligent Envelopes for High-Performance Buildings, Springer International Publishing, Cham, 2017, https://doi.org/10.1007/978-3-319-39255-4.

[5] M.D. Knudsen, S. Petersen, Economic model predictive control of space heating and dynamic solar shading, Energy Build. 209 (2020), 109661, https://doi.org/10.1016/j.enbuild.2019.109661.

[6] M. Dabbagh, M. Krarti, Evaluation of the performance for a dynamic insulation system suitable for switchable building envelope, Energy Build. 222 (2020), 110025, https://doi.org/10.1016/j.enbuild.2020.110025.

[7] B.P. Jelle, Traditional, state-of-the-art and future thermal building insulation materials and solutions – properties, requirements and possibilities, Energy Build. 43 (2011) 2549–2563, https://doi.org/10.1016/j.enbuild.2011.05.015.

[8] B.P. Jelle, A. Gustavsen, R. Baetens, The path to the high performance thermal building insulation materials and solutions of tomorrow, J. Build. Phys. 34 (2010) 99–123, https://doi.org/10.1177/1744259110372782.

[9] A.M. Papadopoulos, State of the art in thermal insulation materials and aims for future developments, Energy Build. 37 (2005) 77–86, https://doi.org/10.1016/j.enbuild.2004.05.006.

[10] O.T. Masoso, L.J. Grobler, A new and innovative look at anti-insulation behaviour in building energy consumption, Energy Build. 40 (2008) 1889–1894, https://doi.org/10.1016/j.enbuild.2008.04.013.

[11] T. Pflug, T.E. Kuhn, R. Nörenberg, A. Glück, N. Nestle, C. Maurer, Closed translucent façade elements with switchable U -value—a novel option for energy management via the facade, Energy Build. 86 (2015) 66–73, https://doi.org/10.1016/j.enbuild.2014.09.082.

[12] M. Dabbagh, M. Krarti, Experimental evaluation of the performance for switchable insulated shading systems, Energy Build. 256 (2022), 111753, https://doi.org/10.1016/j.enbuild.2021.111753.

[13] C. Maurer, N. Nestle, T. Pflug, F. Prissok, A. Hafner, F. Schneider, Concept for adaptive wall elements with switchable U-and g-value. https://www.researchgate.net/publication/326573078, 2018.

[14] B. Park, W.v. Srubar, M. Krarti, Energy performance analysis of variable thermal resistance envelopes in residential buildings, Energy Build. 103 (2015) 317–325, https://doi.org/10.1016/j.enbuild.2015.06.061.

[15] K. Menyhart, M. Krarti, Potential energy savings from deployment of Dynamic Insulation Materials for US residential buildings, Build. Environ. 114 (2017) 203–218, https://doi.org/10.1016/j.buildenv.2016.12.009.

[16] M.S. Sodha, J.K. Nayak, N.K. Bansal, I.C. Goyal, Thermal performance of a solarium with removable insulation, Build. Environ. 17 (1982) 23–32, https://doi.org/10.1016/0360-1323(82)90006-3.

[17] H. Cui, M. Overend, A review of heat transfer characteristics of switchable insulation technologies for thermally adaptive building envelopes, Energy Build. 199 (2019) 427–444, https://doi.org/10.1016/j.enbuild.2019.07.004.

[18] N. Nestle, T. Pflug, C. Maurer, F. Prissok, A. Hafner, F. Schneider, Translucent wall elements with switchable U - and g -value, Ce/Papers 2 (2018) 245–253, https://doi.org/10.1002/cepa.927.

[19] M. Krzaczek, Z. Kowalczuk, Thermal Barrier as a technique of indirect heating and cooling for residential buildings, Energy Build. 43 (2011) 823–837, https://doi.org/10.1016/j.enbuild.2010.12.002.

[20] H. Cui, M. Overend, A review of heat transfer characteristics of switchable insulation technologies for thermally adaptive building envelopes, Energy Build. 199 (2019) 427–444, https://doi.org/10.1016/j.enbuild.2019.07.004.

[21] M. Kimber, W.W. Clark, L. Schaefer, Conceptual analysis and design of a partitioned multifunctional smart insulation, Appl. Energy 114 (2014) 310–319, https://doi.org/10.1016/j.apenergy.2013.09.067.

[22] F. Stazi, A. Vegliò, C. di Perna, P. Munafò, Retrofitting using a dynamic envelope to ensure thermal comfort, energy savings and low environmental impact in Mediterranean climates, Energy Build. 54 (2012) 350–362, https://doi.org/10.1016/j.enbuild.2012.07.020.

[23] A. Berge, C.-E. Hagentoft, P. Wahlgren, B. Adl-Zarrabi, Effect from a variable U-value in adaptive building components with controlled internal air pressure, Energy Proc. 78 (2015) 376–381, https://doi.org/10.1016/j.egypro.2015.11.677.

[24] B.P. Jelle, Traditional, state-of-the-art and future thermal building insulation materials and solutions – properties, requirements and possibilities, Energy Build. 43 (2011) 2549–2563, https://doi.org/10.1016/j.enbuild.2011.05.015.

[25] E. Cuce, P.M. Cuce, C.J. Wood, S.B. Riffat, Toward aerogel based thermal superinsulation in buildings: a comprehensive review, Renew. Sustain. Energy Rev. 34 (2014) 273–299, https://doi.org/10.1016/j.rser.2014.03.017.

[26] Venture Partners at CU Boulder, Switchable Phase Change Material Systems for Building Envelopes, University of Colorado Boulder, 2021. https://www.colorado.edu/venturepartners/2021/11/17/switchable-phase-change-material-systems-building-envelopes. (Accessed 17 October 2022).

[27] M. Fawaier, B. Bokor, Dynamic insulation systems of building envelopes: a review, Energy Build. 270 (2022), 112268, https://doi.org/10.1016/j.enbuild.2022.112268.

[28] M. Knoop, O. Stefani, B. Bueno, B. Matusiak, R. Hobday, A. Wirz-Justice, K. Martiny, T. Kantermann, M. Aarts, N. Zemmouri, S. Appelt, B. Norton, Daylight: what makes the difference? Light. Res. Technol. 52 (2020) 423–442, https://doi.org/10.1177/1477153519869758.

[29] S. Nishikawa, I. Gomi, S. Katsumata, H. Kamata, A. Nagata, T. Kinoshita, E. Sakuma, Experimental and numerical study of heat transfer from a window with an internal Venetian blind, Energy Build. 223 (2020), 110128, https://doi.org/10.1016/j.enbuild.2020.110128.
[30] Y. Sun, Y. Wu, R. Wilson, S. Lu, Experimental measurement and numerical simulation of the thermal performance of a double glazing system with an interstitial Venetian blind, Build. Environ. 103 (2016) 111–122, https://doi.org/10.1016/j.buildenv.2016.03.028.
[31] X. Liu, Y. Sun, S. Wei, L. Meng, G. Cao, Illumination distribution and daylight glare evaluation within different windows for comfortable lighting, Results in Optics 3 (2021), 100080, https://doi.org/10.1016/j.rio.2021.100080.
[32] F. Abd-Alhamid, M. Kent, Y. Wu, Quantifying window view quality: a review on view perception assessment and representation methods, Build. Environ. 227 (2023), 109742, https://doi.org/10.1016/j.buildenv.2022.109742.
[33] E. Sorooshnia, M. Rashidi, P. Rahnamayiezekavat, B. Samali, Optimizing window configuration counterbalancing energy saving and indoor visual comfort for sydney dwellings, Buildings 12 (2022) 1823, https://doi.org/10.3390/buildings12111823.
[34] R. Tällberg, B.P. Jelle, R. Loonen, T. Gao, M. Hamdy, Comparison of the energy saving potential of adaptive and controllable smart windows: a state-of-the-art review and simulation studies of thermochromic, photochromic and electrochromic technologies, Sol. Energy Mater. Sol. Cell. 200 (2019), 109828, https://doi.org/10.1016/j.solmat.2019.02.041.
[35] H. Alkhatib, P. Lemarchand, B. Norton, D.T.J. O'Sullivan, Comparison of control parameters for roller blinds, Sol. Energy 256 (2023) 110–126, https://doi.org/10.1016/j.solener.2023.03.042.
[36] J. Wienold, J. Christoffersen, Evaluation methods and development of a new glare prediction model for daylight environments with the use of CCD cameras, Energy Build. 38 (2006) 743–757, https://doi.org/10.1016/j.enbuild.2006.03.017.
[37] C. Pierson, J. Wienold, M. Bodart, Daylight discomfort glare evaluation with evalglare: influence of parameters and methods on the accuracy of discomfort glare prediction, Buildings 8 (2018) 94, https://doi.org/10.3390/buildings8080094.
[38] S. Daich, M.Y. Saadi, B.E. Piga, A.M. Daiche, A combined method for an exhaustive investigation of the anidolic ceiling effect on improving indoor office daylight quality: an approach based on HDR photography and subjective evaluations, Journal of Daylighting 8 (2021) 149–164, https://doi.org/10.15627/jd.2021.14.
[39] M. Wetter, Generic optimization program user manual version 3.0.0, berkeley, California (United States). https://doi.org/10.2172/962948, 2009.
[40] R. Tällberg, B.P. Jelle, R. Loonen, T. Gao, M. Hamdy, Comparison of the energy saving potential of adaptive and controllable smart windows: a state-of-the-art review and simulation studies of thermochromic, photochromic and electrochromic technologies, Solar Energy Materials and Solar Cells, 200, https://doi.org/10.1016/j.solmat.2019.02.041, 2019.
[41] J. Mäkitalo, Simulating control strategies of electrochromic windows. https://www.diva-portal.org/smash/get/diva2:678505/fulltext01.pdf, 2013.
[42] J. Haarhoff, E.H. Mathews, A Monte Carlo method for thermal building simulation, Energy Build. 38 (2006) 1395–1399, https://doi.org/10.1016/j.enbuild.2006.01.009.
[43] M.J. Sørensen, S.H. Myhre, K.K. Hansen, M.H. Silkjær, A.J. Marszal-Pomianowska, L. Liu, Integrated building energy design of a Danish office building based on Monte Carlo simulation method, Energy Proc. 132 (2017) 93–98, https://doi.org/10.1016/j.egypro.2017.09.646.
[44] T. Østergård, R.L. Jensen, F.S. Mikkelsen, The best way to perform building simulations? One-at-a-time optimization vs. Monte Carlo sampling, Energy Build. 208 (2020), 109628, https://doi.org/10.1016/j.enbuild.2019.109628.
[45] A. Ghosh, B. Norton, T.K. Mallick, Daylight characteristics of a polymer dispersed liquid crystal switchable glazing, Sol. Energy Mater. Sol. Cell. 174 (2018) 572–576, https://doi.org/10.1016/j.solmat.2017.09.047.
[46] American society of heating refrigerating and air-conditioning engineers, standard 62.1-2016 – ventilation for acceptable indoor air quality. https://www.techstreet.com/ashrae/standards/ashrae-62-1-2016?product_id=1912838, 2019. (Accessed 23 December 2022).
[47] American society of heating refrigerating and air-conditioning engineers, thermal environmental conditions for human occupancy. https://www.ashrae.org/technical-resources/bookstore/standard-55-thermal-environmental-conditions-for-human-occupancy, 2020.
[48] C. Ticleanu, Lighting in the workplace – is it just about vision, 1–30, https://iosh.com/media/4142/iosh-2019-cosmin-ticleanu.pdf, 2019.
[49] British Standards Institute, BS EN 17037 daylighting of buildings. https://www.bsigroup.com/en-GB/industries-and-sectors/construction-and-building/bs-en-17037-daylighting-of-buildings/, 2018. (Accessed 22 December 2022).
[50] A. Ghosh, B. Norton, A. Duffy, Daylighting performance and glare calculation of a suspended particle device switchable glazing, Sol. Energy 132 (2016) 114–128, https://doi.org/10.1016/j.solener.2016.02.051.
[51] Ashrae, International weather for energy calculation (IWEC) files. https://www.ashrae.org/technical-resources/bookstore/ashrae-international-weather-files-for-energy-calculations-2-0-iwec2, 2021. (Accessed 25 March 2021).
[52] S. Rupp, M. Krarti, Analysis of multi-step control strategies for dynamic insulation systems, Energy Build. 204 (2019), 109459, https://doi.org/10.1016/j.enbuild.2019.109459.
[53] M.J.N. Oliveira Panão, S.M.L. Camelo, H.J.P. Gonçalves, Solar load ratio and ISO 13790 methodologies: indirect gains from sunspaces, Energy Build. 51 (2012) 212–222, https://doi.org/10.1016/j.enbuild.2012.05.019.
[54] L.S. Poteat, M.K. Sharp, Solar load ratio parameters for a passive solar heat pipe system, in: American Society of Mechanical Engineers, 2015, https://doi.org/10.1115/ES2015-49136.
[55] R. Bruno, P. Bevilacqua, D. Cirone, S. Perrella, A. Rollo, A calibration of the solar load ratio method to determine the heat gain in PV-trombe walls, Energies 15 (2022) 328, https://doi.org/10.3390/en15010328.